# Pavement Texture and Its Wave-Scattering Properties: Application to Light Reflectance and Skid Resistance

A. L. KAZAKOV

**The reflectivity characteristics of a road surface are crucial to the luminance design of highway lighting systems. At present, the reflectance matrices used for design calculations are obtained by experimental procedure and contain important information about the pavement surface texture. In this paper is described model built on the theory of dispersion of electromagnetic waves by random rough surfaces in a high-frequency approximation, as applied to pavements. The model explains the reflectance properties of pavements on the basis of the statistical characteristics of the surface texture and the physical properties of the pavement mix. To test the model, measurements were done on the Ontario road reflectance matrix photometer at the University of Toronto. When tested and calibrated, the model showed good agreement between predicted and measured data. The backscattering of ultrasonic waves by pavement surfaces is discussed in terms of low-frequency approximation of the theory of scattering from random rough surfaces. Simple experiments, using scale models, showed good correlation between the intensity of backscattering from the pavement surface and its skid resistance. The model can be used to extract statistical surface texture characteristics from experimental data for the assessment of other properties of pavements, such as skid resistance or pavement wear.**

In Proposed American National Standard Practice for Roadway Lighting *(1)*, the Illuminating Engineering Society (IES) recommended the luminance method of highway lighting design. The light reflectance properties of the pavement surface are key factors in the suggested design procedure. Reflectivity measurements made from a highway core sample are used to classify the pavement into one of four reflectivity classes. In simulating the viewing angle of the driver, measurements must be made at an angle of 1 degree to the core's surface. The data obtained in such measurements contain only limited information on pavement surface texture characteristics. Measurements at this low angle of reflectance are tedious and require a laboratory setting to obtain the desired accuracy *(1,2)*.

The use of a higher angle of reflection for the measurements simplifies the measuring procedure and, in conjunction with the developed model, makes possible calculation of the 1-degree reflectivity values with desirable accuracy. Moreover, the data from such measurements can be used to obtain other important pavement surface characteristics such as skid resistance and pavement wear.

Research and Development Branch, Ontario Ministry of Transportation and Communications, Central Building, Room 331, 1210 Wilson Avenue, Downsview, Ontario M3M 1J8, Canada.

A mathematical model, based on the theory of reflection of electromagnetic waves from random rough surfaces, was developed and tested to transform the reflectivity values, measured at a large angle of reflection, and to obtain the pavement surface characteristics. This model makes possible the prediction of reflectivity values for different reflection angles from given statistical characteristics of the pavement surface texture. Conversely, the model makes possible determination of pavement surface statistical characteristics from the reflection measurements at large angles of reflection.

The derivation of the model is explained and the findings obtained with limited available experimental data are described in this paper.

The developed model can be used to

1. Estimate the statistical characteristics of pavement surface texture using the reflectance data,
2. Predict the reflectivity values of a surface from given surface texture characteristics, and
3. Convert the reflectivity values obtained for a high angle of reflectance to an angle of 1 degree, or other angles of reflection that might be more suitable for evaluation of a highway lighting installation from, for example, the point of view or angle of vision of a truck driver.

In the next section information is provided on the luminance concept of highway lighting design and the measurement parameters and procedures for total assessment of the problem. This information is necessary for comparison of experimental data with results obtained from the model.

## CONCEPTS OF LUMINANCE

The design of roadway lighting systems, based on the luminance concept, takes into account the amount of light reflected from the road surface toward the driver. This standard design procedure supersedes the well-known illuminance, or incident light, design technique.

The procedure for determining the amount of light reflected by the road surface involves summing the intensity of light from each luminaire reflected by the pavement surface toward the driver. The road geometry and pertinent notation are shown in Figure 1. A grid system is used for referencing points on the road. At each grid point the incident illumination for each luminaire [$E_{oi}$(cd/m$^2$)] is determined, and the contribution to total luminance by a particular luminaire [$L_i$(cd/m$^2$)] is calculated using

$$L_i = E_{oi} \times q(\alpha, \beta, \gamma, \delta) \quad (1)$$

where q is the directional reflectance coefficient.

The value of q is a function of the angles of incidence ($\gamma$ and $\delta$) and the angles of reflection ($\alpha$ and $\beta$). These angles are defined in Figure 1.

The total luminance of Point P on the road then is

$$L_p = \Sigma L_i \quad (2)$$

It is assumed that the driver views straight ahead; thus the angle $\delta$ is zero degrees.

If the value of $E_{oi}$ is considered in terms of intensity ($I_i$) of the luminaire (light source), the following relationship obtains:

$$E_{oi} = I_i(\phi, \gamma) \cos/D_i^2 \quad (3)$$

where $D_i^2 = h^2/\cos^2 \gamma$ and $\phi$, $\gamma$, and h are as defined in Figure 1.

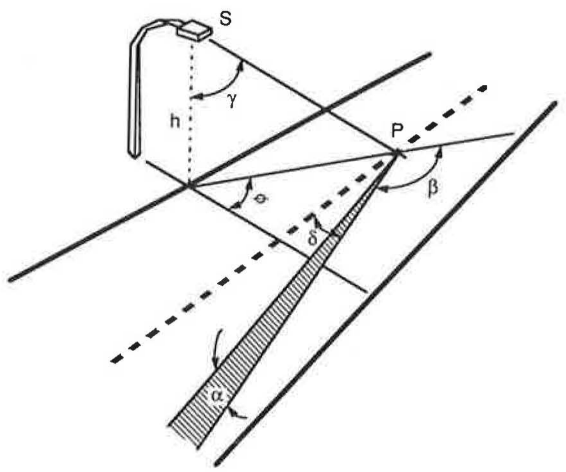


**FIGURE 1 Road geometry.**

Substitution of $E_{oi}$ and $D_i$ into Equation 1 defines the luminance as a product of factors that depend on the reflective properties of the pavement and lighting design parameters (for $\delta$ = 0 degree):

$$L_i = q(\gamma, \alpha, \beta) \times I_i(\phi, \gamma) \times \cos^3 \gamma/h^2 \quad (4)$$

The reduced reflectance coefficient is defined as

$$r = q(\gamma, \alpha, \beta) \cos^3 \gamma \quad (5)$$

Substituting r simplifies Equation 4 to

$$L_i = r(\gamma, \alpha, \beta) \times I_i(\phi, \gamma)/h^2 \quad (6)$$

and the total luminance of Point P is

$$L_p = \Sigma r(\gamma, \alpha, \beta) \times I_i(\phi, \gamma)/h^2 \quad (7)$$

The Comité International d'Eclairage (CIE) has recommended and published standard reflectance tables *(1)*. These tables represent four standard surfaces that are currently used in highway lighting design. The tables *(1,* Table 1) represent r-values for $\alpha$ = 1 degree and $\delta$ = 0 degree. The actual reflectance matrices obtained from the measurement are only used to classify the pavement surface into one of the standard classes.

The value of the directional reflectance coefficient [$q(\alpha, \beta, \gamma, \delta)$] for each value of the arguments depends on the statistical properties of the surface geometry, or texture, and the effective optical properties of the pavement mix. The theory of reflection of electromagnetic waves from random rough surfaces can be applied to describe this dependence and to model the reflectance properties of the pavement for different angles of reflectance.

The statistical characteristics of a pavement surface texture are not readily available. Different experimental techniques were recently developed to obtain the texture characteristics used in skid prediction models. The developed model can be used to derive these characteristics from the directional reflectance coefficient measured at a high angle of light reflectance (30 degrees in the present study). The texture characteristic thus obtained can be used to calculate the reflectance matrices for the pavement as well as other pavement properties that depend on texture.

## MEASUREMENT PROCEDURE

Measurement of the reflectance matrixes for a high angle of reflectance was done on the Ontario road reflectance matrix photometer at the University of Toronto. The standard procedure of measurement for 1-degree angle of reflectance is described in detail by Jung et al. *(2,3)*. The instrumentation was adjusted and calibrated for measurement at the 30-degree reflectance angle.

The experimental setup for this measurement is shown in Figure 2. A photometer (M) measures the luminance of a sample from a constant angle of view $\alpha$ = 30 degrees. The constant-intensity ($I_0$) light source (S) moves along a rail (AB) at a constant height (h) above the core sample. The photometer and the sample are rotated together around the axis A-A, and automatic readings of the photometer output are taken at specified angles ($\beta$) of rotation starting from 0 degree and continuing up to 165 degrees. The geometry of the instrument did not

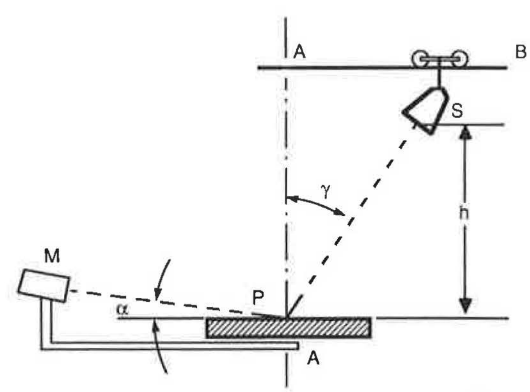


**FIGURE 2 Ontario road reflectance matrix photometer.**

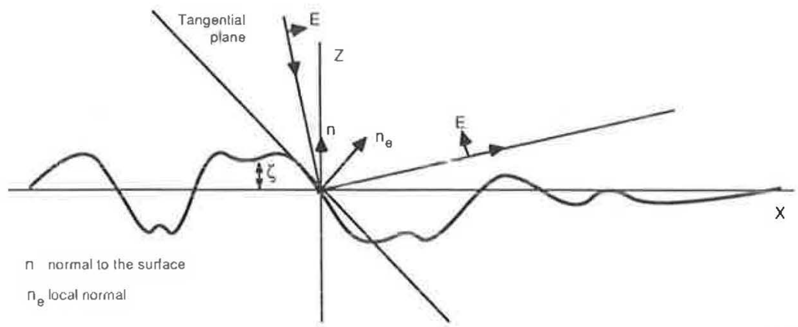


**FIGURE 3 Two-dimensional representation of mirror reflection by tangential plane.**

allow for measurements at $\beta$ = 180 degrees with a 30-degree angle of reflection, so $\beta$ = 165 degrees was the maximum rotation angle used in experiments *(4)*.

The reduced reflectance coefficient (r) for each geometry of measurement is determined by rearranging Equation 4:

$$r = L\,h^2/I_0 \tag{8}$$

where L is luminance measured in a particular direction and h and $I_0$ are experimental parameters defined previously. The directional reflectance coefficient (q) can then be determined as $q = r/\cos^3 \gamma$.

## DEVELOPMENT OF THE MODEL

The solution of the problem of scattering of waves by flat rough surfaces that have a texture smaller than the wavelength was given by Lord Rayleigh as early as 1896 in his classical monograph *The Theory of Sound (5)*. Later, the practical problems of radar technology (scattering of electromagnetic waves by the surface of the earth) led to a broad attack on the problems of the scattering of electromagnetic waves by rough surfaces. The perturbation solution for a mildly sloping texture was suggested by Feinberg *(6)* and Rice *(7)*; the problem of wave scattering by a random surface with irregularities larger than the wavelength was solved by Brekhovskikh *(8)*.

These first attacks on the problem were later extended to include cases of boundaries with finite conductivity *(9)* and boundaries with randomly varying impedance (10). Later workers extended understanding to more realistic surface textures, such as a combination of large irregularities (in comparison with wavelength) and the overlaying microtexture *(11,12)*. Different physical and mathematical methods were used in an effort to closely model reality and find better approximations. Monographs *(13,14)* present reviews of these investigations.

Similar results were obtained by investigators who approached the same problem from different physical perspectives. The present author mainly follows the works of Isakovich *(9)*, Semenov *(12)*, and Sancer *(15)*, which are based on one of the main approaches to the problem of scattering of waves—the Kirchgoff approximation and the Kirchgoff vector integral equation *(16)*.

In modeling the scattering of light by a pavement surface, it is assumed that the surface is flat on the average and that surface irregularities are much larger than the wavelength of the light (i.e., high-frequency approximation can be used). The latter assumption is supported by scanning electron microscopy analysis of different road aggregate materials *(17)*.

Pavement is assumed to be homogeneous in its constitutive properties. This assumption is based on the work of Bass *(10)*, who showed that for mixes with randomly distributed materials the effective value of the pertinent properties of materials can be used. In this model, estimation of the light intensity scattered into the particular direction is done, effectively, by summation of mirror reflections from each element of the surface (Figure 3). The value of this sum averaged over the ensemble represents the final result of the calculations.

The model takes into account the effect of shadowing of one part of the surface by another, which is important for grazing angles of scattering. In Figure 4 the effect of shadowing of the incident and reflected light is shown. For surfaces with irregularities much larger than the wavelength of the light, the effect of secondary reflections is proven to be negligible.

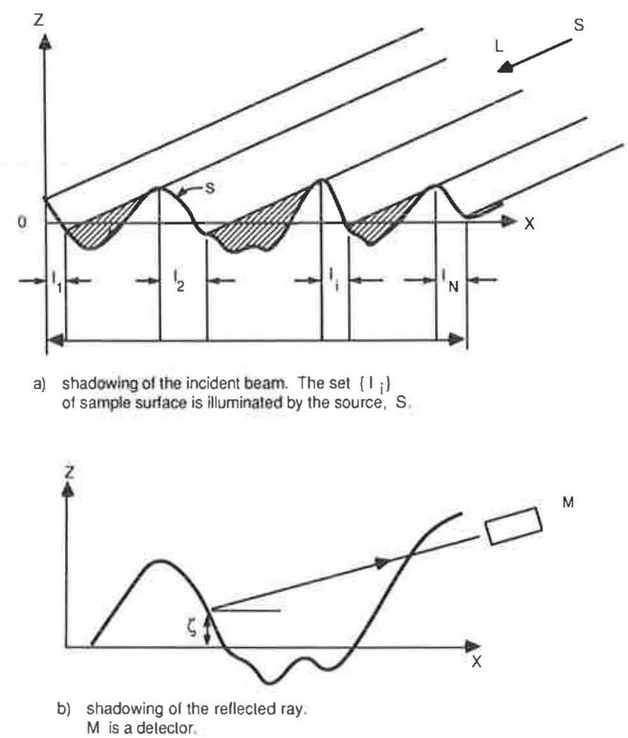


**FIGURE 4 Representation of shadowing.**

In mathematical terms the pavement surface is represented as a realization of the random function $z = \zeta(x,y)$. The Kirchgoff approximation is used to calculate the field on the surface ($\vec{E}_s$) as the sum of the incident field ($\vec{E}_o$) and the field reflected (scattered) from the plane tangential to the surface at any given point ($\vec{E}_t$): $\vec{E}_s = \vec{E}_o + \vec{E}_t$. The reflected component of the surface field ($\vec{E}_t$) can be presented as a function of the incident field using the Fresnel reflection coefficients (M and N), which are specified hereafter. Thus the field on the sample surface can be calculated given the incident electric ($\vec{E}_o$) and magnetic ($\vec{H}_o$) fields and the effective values of material properties: dielectric constant ($\varepsilon$) and magnetic susceptibility ($\mu$). Kirchgoff's integral is then applied to determine the field ($\vec{E}$) at the receiver from the field known on the enclosed surface. The electromagnetic field intensity, which is proportional to the square of the modulus of the electric field vector ($|\vec{E}^2|$), is then estimated and its ensemble average is the final result of the derivations. The following formulas are after Sancer *(15)*:

$$J = <|\vec{E}^2|> = (|\vec{E}_o^2|/R_o^2)\, S(a_1/a_4)\, (|M|^2 + |N|^2)\, W_1 W_2 \quad (9)$$

where

- $J$ = the ensemble average of the intensity of scattered light,
- $R_o$ = distance from source to the surface,
- $S$ = scattering area of a sample,

$$a_1 = 1 - \sin\gamma \cos\alpha \cos\phi \cos\gamma \ \sin\alpha, \quad (10)$$

$$a_4 = \cos\gamma + \sin\alpha, \quad (11)$$

$$N = [\varepsilon \cos\theta - (\mu\varepsilon - \sin^2\theta)^{1/2}]/[\varepsilon \cos\theta + (\mu\varepsilon \sin^2\theta)^{1/2}], \quad (12)$$

$$M = [\mu \cos\theta - (\mu\varepsilon - \sin^2\theta)^{1/2}]/[\mu \cos\theta + (\mu\varepsilon \sin^2\theta)^{1/2}], \quad (13)$$

$$\cos\theta = [(1 - \cos\alpha \sin\gamma \cos\phi + \sin\alpha \cos\gamma)/2]^{1/2}, \text{ and} \quad (14)$$

$\theta$ = the local angle of incidence.

$W_1$ is the joint probability density function of the partial derivatives of the random function $z = \xi(x,y)$; $W_1(\xi_x, \xi_y)$ is evaluated at the values of $\xi_x = (\cos\alpha - \sin\gamma\cos\phi)/a_4$ and $\xi_y = \sin\gamma \sin\phi/a_4$ or, in other words, for the mirror reflection of the incident light toward the receiver. The validity of Equation 9 is not limited to normal, Gaussian, random surfaces. However, a Gaussian stationary isotropic random function is used to compare the results of the model with those of the experiments. Thus the joint probabilities distribution of x and y components of the gradient of the surface $\xi(x,y)$, which is denoted as $W_1(\xi_x, \xi_y)$, is normal and can be written as

$$W_1 = (2\pi <\alpha^2>) \exp[-(\xi_x^2 + \xi_y^2)/(2 <\alpha^2>)] \quad (15)$$

$$RMSS = <\alpha^2> \quad (16)$$

RMSS is the root mean square slope of the surface.

$W_2$ is a conditional probabilities function that corrects the results for shadowing. It takes into account shadowing of the incident and reflected rays by an isotropic, normally distributed surface. $W_2$ is the product of the probability of an incident ray hitting a given point on the surface, given a certain inclination at that point, and the probability of a ray reflected from a given point reaching the observer. These probabilities account for the nonshadowing of the incident and scattered fields by the surface.

$$\begin{aligned} W_2 &= (C_0 + 1) && \text{for } \alpha > \gamma \text{ and } \beta = 0 \text{ or } 180 \\ W_2 &= (C_2 + 1) && \text{for } \alpha < \gamma \text{ and } \beta = 0 \text{ or } 180 \\ W_2 &= (C_0 + C_2 + 1) && \text{in any other case} \end{aligned} \quad (17)$$

where

$$2\,C_0 = (2\,|<\alpha^2>|/\pi) \tan\gamma \exp[-\cot^2\gamma/(2|<\alpha^2>|)] - \operatorname{erfc}[\cot\gamma/(2|<\alpha^2>|)^{1/2}] \quad (18)$$

$$2\,C_2 = (2\,|<\alpha^2>|/\pi) \tan\alpha \exp[-\cot^2\alpha/(2|<\alpha^2>|)] - \operatorname{erfc}[\cot\alpha/(2|<\alpha^2>|)^{1/2}] \quad (19)$$

where $\operatorname{erfc}(x) = 1 - 2/\pi^{1/2} \int_0^x \exp(-x^2)dx$ is a well-known function of errors *(18)*.

The power scattered in any direction by a random rough surface can be calculated (in the high-frequency limit) if the statistical properties of the surface texture are given. To compare model results with measured pavement reflectance data, Equation 9 is rewritten as

$$J = A\,[I_0/(4\pi R_o^2 \rho^2)]\, F \exp(-Bx)\, W_2 \quad (20)$$

where

$$A = S\,\pi(1/<\alpha^2>), \quad (21)$$

$$F = (a_1/a_4)(|M|^2 + |N|^2), \quad (22)$$

$$x = (2\,a_1/a_4^2) - 1, \quad (23)$$

$$I_0 = (4\pi R_o^2)\,|\vec{E}_o^2|, \quad (24)$$

$$B = 1/(2 <\alpha^2>), \text{ and} \quad (25)$$

$\rho$ = distance from the surface to the receiver.

Furthermore, considering the illuminance (E) with respect to the source intensity ($I_0$):

$$E = (I_0/4\pi R_o^2) \cos\gamma \quad (26)$$

and the relationship between field intensity and luminance (L):

$$J = L/(\rho^2) \quad (27)$$

a model for the reflectance coefficient can be derived. Using Equations 1, 5, 26, and 27 gives

$$J = (I_0\, r)/(4\pi R_o^2 \rho^2 \cos^2\gamma) \quad (28)$$

Equating 20 and 28 yields the following relationship:

$$r = A \cos^2 \gamma F \exp(-Bx) W_2 \quad (29)$$

This expression explicitly defines reduced reflectance coefficients through the parameters of the physical model for every geometry.

By introducing $r' = r/(F \cos^2 \gamma)$, Equation 29 can be rewritten in a form more suitable for further regression analysis:

$$r' = A \exp(-Bx) W_2 \quad (30)$$

Assuming that the effective values of the dielectric constant of the scattering surface material are known, the values F and x are defined for any geometry of measurements; A and B are regression parameters that depend on the texture; and $W_2$ is a shadowing factor, described previously. As may be seen from Equations 17–19, $W_2$ depends on the geometry of scattering and root mean square slope of the surface texture. Using the experimental values of reduced reflectance coefficients of pavement, measured at a 30-degree angle of reflection, the root mean square slope of the texture and the constant A were found by an iterative least square procedure.

In the first step of iteration, the shadowing factor ($W_2$) was assumed to be negligible ($W_2 = 1$) for the purpose of obtaining the constants (A and B) of Expression 30. $W_2$ was then estimated using the value of root mean square slope from the first iteration. Experimental data were adjusted to eliminate the shadowing effect by multiplication of the reflectance matrix by the inverse shadowing factor. When this technique was used, the process converged within three to four iterations.

The values of effective constitutive properties of the pavement mix ($\varepsilon$ and $\mu$) are localized within a narrow range. It was assumed that the pavement mix was not magnetic, so magnetic permeability ($\mu$) was set equal to unity. Electric susceptibility of the mix was assumed to be in the range of 1.5 to 5. This estimate was considered correct because only dielectric highway core samples were dealt with. To investigate the effect of change in these values on the model results, a sensitivity analysis was performed that showed that the model was not very sensitive to changes in the effective value of electric permeability within a given range. This was due, in part, to the high angle of reflection used—really, the value of $|M|^2 + |N|^2$ that, depending on the dielectric permeability ($\varepsilon$) and the local angle of incidence ($\theta$), is almost a constant for angles of incidence below about 60 degrees. For the 30-degree reflection measurements, local angle of incidence, corresponding to mirror reflection toward the receiver, was for almost all r-values measured below 60 degrees.

## DISCUSSION OF RESULTS

Figures 5 and 6 show the influence of the root mean square slope of the surface on its light reflectance property (r) as it is accounted for by the model. The graphs presented are based on the values of calculated reduced reflectance coefficients. These calculations were done for the case of direct and backward scattering angles $\phi = 90$ degrees and $-90$ degrees, respectively. In other words, the receiver is in the plane of the incident ray and the normal to the average surface plane ($\vec{n}$). In addition, the graphs present the case of 90-degree scattering with the angle $\theta = 0$. The different parameters used in the calculation are given in the legends to Figures 5 and 6.

For almost flat surfaces, with a small value of RMSS (≈0.10 to 0.25), the reflection is almost mirrorlike. The reduced reflectance coefficient sharply decreases when the angles of scattering deviate from the angle of mirror reflection, equal to 30 degrees for Figure 5 and 1 degree for Figure 6. With increased surface roughness, the value of RMSS is increased and more diffuse, and a broader scattering of light is observed. At the same time, with an increase in RMSS value the maximum of reduced reflection coefficient is shifted from the angle of mirror reflection to a larger angle ($\gamma$) and then for an angle $\phi = -90$ degrees. Thus a maximum reduced reflection coefficient is observed for a backscattering of light. The same effects are observed for the scattering of light in all directions. The shadowing of one part of the surface by another narrows the directional distribution of light scattering and shifts the maximum r-values toward the angle of mirror reflection.

The experimental reflectance matrix is given in Table 1 for measurements with a 30-degree viewing angle. These data were used to obtain the root mean square slope of the pavement

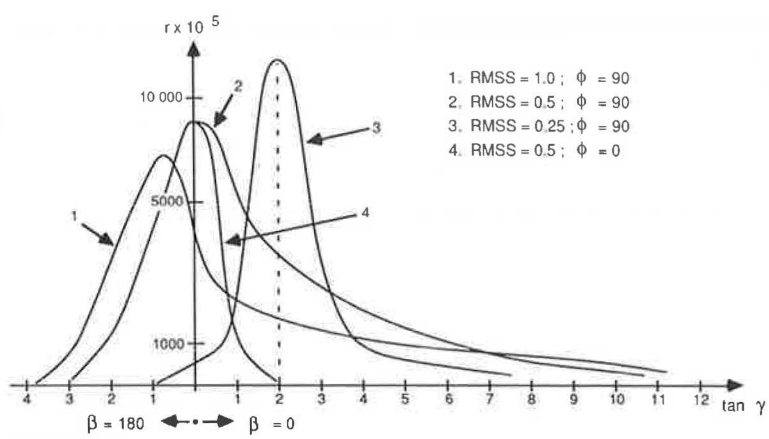


**FIGURE 5 Angular characteristic of light scattering for reflectance angle of 30 degrees ($\gamma$, $\beta$, and $\phi$ angles as defined in Figure 1).**

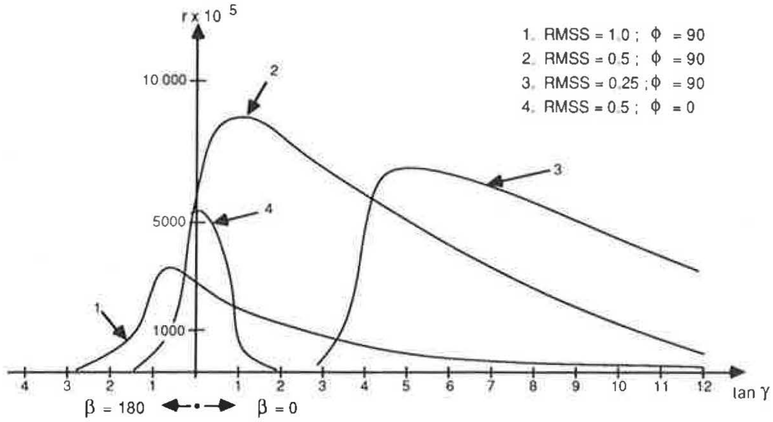


**FIGURE 6 Angular characteristic of light scattering for reflectance angle of 1 degree (γ, β, and φ angles as defined in Figure 1).**

**TABLE 1 MEASURED REFLECTANCE COEFFICIENTS (x $10^4$) FOR 30-DEGREE ANGLE OF REFLECTION**

| 0 | 2 | 5 | 10 | 15 | 20 | 25 | 30 | 45 | 60 | 75 | 90 | 105 | 120 | 135 | 150 | 165 |
|---|---|---|---|---|---|---|---|---|---|---|---|---|---|---|---|---|
| 788 | 794 | 787 | 792 | 789 | 786 | 788 | 785 | 795 | 792 | 797 | 796 | 792 | 792 | 786 | 783 | 783 |
| 848 | 845 | 851 | 855 | 851 | 846 | 843 | 833 | 819 | 797 | 761 | 748 | 721 | 710 | 688 | 683 | 674 |
| 822 | 822 | 822 | 822 | 808 | 796 | 785 | 762 | 705 | 653 | 615 | 592 | 557 | 541 | 521 | 523 | 517 |
| 742 | 747 | 764 | 734 | 714 | 693 | 666 | 634 | 561 | 498 | 458 | 420 | 403 | 393 | 387 | 386 | 386 |
| 648 | 649 | 649 | 631 | 603 | 561 | 527 | 491 | 408 | 360 | 322 | 298 | 284 | 278 | 273 | 278 | 283 |
| 564 | 566 | 557 | 531 | 500 | 452 | 414 | 372 | 305 | 261 | 230 | 213 | 200 | 200 | 202 | 203 | 208 |
| 485 | 488 | 480 | 442 | 400 | 361 | 321 | 295 | 229 | 192 | 167 | 155 | 150 | 146 | 149 | 153 | 159 |
| 417 | 416 | 398 | 357 | 320 | 283 | 249 | 224 | 173 | 143 | 126 | 116 | 110 | 110 | 111 | 116 | 125 |
| 350 | 366 | 330 | 297 | 262 | 224 | 194 | 173 | 132 | 110 | 97 | 89 | 85 | 84 | 84 | 90 | 98 |
| 253 | 249 | 240 | 205 | 173 | 143 | 126 | 113 | 80 | 66 | 59 | 53 | 50 | 51 | 53 | 55 | 57 |
| 185 | 184 | 172 | 146 | 121 | 99 | 83 | 76 | 53 | 42 | 38 | 36 | 35 | 35 | 35 | 36 | 38 |
| 137 | 135 | 126 | 107 | 86 | 70 | 58 | 51 | 38 | 31 | 27 | 25 | 23 | 24 | 22 | 25 | 28 |
| 109 | 104 | 97 | 80 | 64 | 53 | 45 | 38 | 27 | 23 | 20 | 20 | 18 | 18 | 18 | 20 | 20 |
| 82 | 81 | 74 | 63 | 51 | 41 | 32 | 27 | 21 | 17 | 16 | 15 | 14 | 14 | 14 | 15 | 15 |
| 66 | 66 | 62 | 48 | 37 | 31 | 27 | 26 | 16 | 14 | 12 | 12 | 12 | 12 | 13 | 13 | 13 |
| 55 | 53 | 50 | 41 | 32 | 25 | 21 | 17 | | | | | | | | | |
| 46 | 44 | 42 | 25 | 27 | 21 | 17 | 15 | | | | | | | | | |
| 38 | 38 | 36 | 30 | 24 | 19 | 14 | 12 | | | | | | | | | |
| 31 | 33 | 30 | 26 | 20 | 15 | 12 | 11 | | | | | | | | | |
| 28 | 28 | 27 | 22 | 18 | 13 | 11 | | | | | | | | | | |
| 24 | 25 | 23 | 20 | 16 | 12 | 10 | | | | | | | | | | |
| 21 | 21 | 20 | 18 | 14 | 11 | 9 | | | | | | | | | | |
| 19 | 19 | 18 | 16 | 14 | 10 | | | | | | | | | | | |
| 17 | 18 | 17 | 15 | 13 | 11 | | | | | | | | | | | |
| 15 | 15 | 15 | 14 | 11 | 9 | | | | | | | | | | | |
| 14 | 14 | 14 | 14 | 12 | 8 | | | | | | | | | | | |
| 13 | 14 | 13 | 13 | 11 | 8 | | | | | | | | | | | |
| 13 | 13 | 13 | 13 | 10 | | | | | | | | | | | | |
| 12 | 12 | 12 | 12 | 10 | | | | | | | | | | | | |

surface using the iterative regression procedure described previously.

Table 2 gives the calculated r-matrix for RMSS = 0.81 for comparison with the experimental data given in Table 1. The calculation of r-matrix is done for $\mu = 1$ and $\varepsilon = 2.5$. To estimate the explanatory power of the model, a correlation coefficient (R) between two sets of r-values was calculated according to Equation 31 and found equal to R = 0.99. This high value of correlation coefficient shows that the directional variability of reduced reflectance coefficient is, to a large extent, encompassed by the developed model:

$$R = [\Sigma(X_i - \bar{X})(Y_i - \bar{Y})]/[\Sigma(X_i - \bar{X})^2\,\Sigma(Y_i - \bar{Y})^2] \qquad (31)$$

Three core samples from the same pavement were used to observe the effect of local variations of roughness and model sensitivity. The RMSS-values estimated by the model from these three sample reflectance matrices were in a narrow range between 0.79 and 0.82.

The theoretical reflectance matrix for a 1-degree viewing angle was then calculated using RMSS-values of the surface estimated from 30-degree measurements. The experimental and calculated r-matrices for 1-degree reflection angle ($\alpha$) are given in Tables 3 and 4, respectively.

The value of the A coefficient of Equation 30 was calculated as a product of the value A obtained from 30-degree measurements and a correction factor. This correction factor (CF) is the result of change in the value of experimental parameters—the surface area seen by the photomultiplier was different for the two sets of measurements, and it was found to be equal to CF = 7.

In comparing the predicted value with the actual data, it was noted that the rate of change of the coefficients, with changes in tan $\gamma$ and $\phi$, is greater in the predicted matrix. As currently

**TABLE 2 CALCULATED REFLECTANCE COEFFICIENTS (x $10^4$) FOR 30-DEGREE ANGLE OF REFLECTION**

| 0 | 2 | 5 | 10 | 15 | 20 | 25 | 30 | 45 | 60 | 75 | 90 | 105 | 120 | 135 | 150 | 165 |
|---|---|---|---|---|---|---|---|---|---|---|---|---|---|---|---|---|
| 741 | 741 | 741 | 741 | 741 | 741 | 741 | 741 | 741 | 741 | 741 | 741 | 741 | 741 | 741 | 741 | 741 |
| 789 | 789 | 788 | 786 | 783 | 779 | 774 | 769 | 748 | 727 | 707 | 690 | 677 | 667 | 660 | 655 | 652 |
| 800 | 799 | 797 | 790 | 778 | 764 | 747 | 730 | 676 | 632 | 599 | 575 | 560 | 548 | 541 | 537 | 535 |
| 788 | 778 | 773 | 754 | 728 | 698 | 666 | 636 | 561 | 508 | 472 | 449 | 434 | 425 | 419 | 416 | 414 |
| 761 | 732 | 719 | 683 | 640 | 597 | 557 | 523 | 443 | 393 | 360 | 340 | 327 | 318 | 312 | 309 | 307 |
| 724 | 669 | 645 | 591 | 537 | 490 | 450 | 417 | 345 | 301 | 273 | 255 | 243 | 235 | 229 | 225 | 223 |
| 682 | 596 | 557 | 493 | 440 | 396 | 360 | 331 | 270 | 232 | 208 | 192 | 181 | 174 | 168 | 164 | 162 |
| 631 | 508 | 464 | 404 | 357 | 319 | 289 | 264 | 212 | 181 | 160 | 146 | 136 | 129 | 124 | 120 | 118 |
| 492 | 413 | 380 | 330 | 290 | 259 | 233 | 212 | 170 | 143 | 125 | 113 | 104 | 97 | 93 | 90 | 88 |
| 318 | 274 | 257 | 224 | 196 | 174 | 157 | 142 | 112 | 92 | 79 | 70 | 63 | 58 | 54 | 52 | 50 |
| 217 | 190 | 179 | 157 | 138 | 122 | 109 | 99 | 77 | 63 | 52 | 45 | 40 | 36 | 33 | 31 | 30 |
| 154 | 137 | 130 | 114 | 100 | 88 | 79 | 72 | 55 | 44 | 36 | 31 | 26 | 24 | 22 | 20 | 19 |
| 114 | 102 | 97 | 85 | 74 | 66 | 59 | 53 | 41 | 32 | 26 | 22 | 18 | 16 | 14 | 14 | 13 |
| 86 | 78 | 74 | 65 | 57 | 51 | 45 | 41 | 31 | 24 | 19 | 16 | 13 | 11 | 10 | 9 | 9 |
| 66 | 60 | 58 | 51 | 44 | 39 | 35 | 32 | 23 | 18 | 14 | 12 | 10 | 8 | 7 | 7 | 6 |
| 53 | 48 | 46 | 40 | 35 | 31 | 28 | 25 | | | | | | | | | |
| 42 | 39 | 37 | 33 | 27 | 25 | 22 | 20 | | | | | | | | | |
| 35 | 32 | 30 | 27 | 23 | 21 | 18 | 17 | | | | | | | | | |
| 29 | 26 | 25 | 22 | 19 | 17 | 15 | 14 | | | | | | | | | |
| 24 | 22 | 21 | 19 | 16 | 14 | 13 | | | | | | | | | | |
| 20 | 19 | 18 | 16 | 14 | 12 | 11 | | | | | | | | | | |
| 17 | 16 | 15 | 14 | 12 | 10 | 9 | | | | | | | | | | |
| 15 | 14 | 13 | 12 | 10 | 9 | | | | | | | | | | | |
| 13 | 12 | 11 | 10 | 9 | 8 | | | | | | | | | | | |
| 11 | 10 | 10 | 9 | 8 | 7 | | | | | | | | | | | |
| 10 | 9 | 9 | 8 | 7 | 6 | | | | | | | | | | | |
| 9 | 8 | 8 | 7 | 6 | | | | | | | | | | | | |
| 8 | 7 | 7 | 6 | 5 | | | | | | | | | | | | |
| 7 | 6 | 6 | 5 | 4 | | | | | | | | | | | | |

**TABLE 3 MEASURED REFLECTANCE COEFFICIENTS (x $10^4$) FOR 1-DEGREE ANGLE OF REFLECTION**

| 0 | 2 | 5 | 10 | 15 | 20 | 25 | 30 | 45 | 60 | 75 | 90 | 105 | 120 | 135 | 150 | 165 |
|---|---|---|---|---|---|---|---|---|---|---|---|---|---|---|---|---|
| 413 | 417 | 413 | 416 | 417 | 417 | 413 | 419 | 423 | 422 | 427 | 422 | 424 | 424 | 418 | 411 | 411 |
| 456 | 461 | 461 | 459 | 456 | 456 | 445 | 449 | 438 | 413 | 403 | 386 | 374 | 363 | 355 | 353 | 349 |
| 482 | 477 | 488 | 477 | 461 | 454 | 433 | 422 | 385 | 344 | 327 | 305 | 291 | 280 | 275 | 279 | 269 |
| 481 | 477 | 475 | 456 | 440 | 413 | 386 | 358 | 301 | 264 | 245 | 229 | 220 | 213 | 211 | 214 | 212 |
| 471 | 472 | 461 | 434 | 386 | 347 | 310 | 278 | 226 | 193 | 169 | 165 | 159 | 156 | 157 | 156 | 160 |
| 455 | 445 | 427 | 371 | 315 | 264 | 233 | 207 | 159 | 140 | 122 | 118 | 118 | 113 | 113 | 117 | 120 |
| 445 | 445 | 403 | 326 | 259 | 213 | 180 | 158 | 116 | 100 | 92 | 89 | 88 | 86 | 91 | 94 | 92 |
| 413 | 403 | 355 | 269 | 208 | 158 | 135 | 110 | 91 | 76 | 69 | 67 | 67 | 71 | 70 | 71 | 76 |
| 395 | 355 | 323 | 226 | 159 | 125 | 101 | 89 | 68 | 61 | 57 | 54 | 54 | 55 | 56 | 60 | 61 |
| 353 | 323 | 246 | 146 | 100 | 78 | 64 | 56 | 43 | 40 | 37 | 36 | 36 | 36 | 40 | 40 | 41 |
| 315 | 280 | 188 | 98 | 65 | 61 | 43 | 38 | 30 | 28 | 25 | 26 | 26 | 26 | 30 | 29 | 31 |
| 280 | 238 | 139 | 69 | 46 | 36 | 31 | 29 | 24 | 22 | 22 | 20 | 20 | 21 | 23 | 23 | 24 |
| 259 | 194 | 104 | 52 | 36 | 28 | 24 | 24 | 18 | 17 | 16 | 16 | 16 | 18 | 19 | 21 | 21 |
| 230 | 162 | 82 | 39 | 26 | 22 | 20 | 17 | 16 | 13 | 13 | 12 | 14 | 14 | 15 | 17 | 17 |
| 209 | 136 | 66 | 32 | 22 | 18 | 15 | 14 | 12 | 12 | 11 | 11 | 12 | 12 | 13 | 14 | 15 |
| 198 | 116 | 52 | 27 | 19 | 15 | 13 | 12 | | | | | | | | | |
| 165 | 101 | 44 | 22 | 16 | 12 | 12 | 10 | | | | | | | | | |
| 174 | 86 | 37 | 18 | 13 | 11 | 10 | 9 | | | | | | | | | |
| 166 | 81 | 32 | 16 | 12 | 10 | 9 | 8 | | | | | | | | | |
| 153 | 65 | 27 | 14 | 10 | 9 | 8 | | | | | | | | | | |
| 144 | 61 | 25 | 13 | 10 | 9 | 7 | | | | | | | | | | |
| 133 | 54 | 23 | 12 | 8 | 7 | 7 | | | | | | | | | | |
| 131 | 49 | 20 | 11 | 8 | 7 | | | | | | | | | | | |
| 124 | 44 | 18 | 10 | 8 | 6 | | | | | | | | | | | |
| 120 | 42 | 17 | 9 | 7 | 6 | | | | | | | | | | | |
| 120 | 38 | 16 | 9 | 7 | 6 | | | | | | | | | | | |
| 117 | 34 | 16 | 8 | 7 | 6 | | | | | | | | | | | |
| 107 | 31 | 13 | 8 | 6 | | | | | | | | | | | | |
| 105 | 29 | 13 | 7 | 6 | | | | | | | | | | | | |

developed, the model considers the surface texture to be normally distributed, with no correlation between the gradient of the microsurface and the height of the microsurface. Because road surfaces are worn down by traveling vehicles, it follows that there would be a greater number of horizontal planes at the top of the microsurface than at the bottom (conceptually, a range of mountains with the tops chopped off might be imagined). This implies that the distribution is skewed and a correlation may exist between the gradient and the height of the microtexture. This would increase the amount of reflection and cause less shadowing, thereby lowering the rate of change.

## SCATTERING OF ULTRASONIC WAVES

The theory of wave scattering by random surfaces was first developed and applied to the scattering of sound. The wavelength of high-frequency ultrasonic waves (about 100 000 Hz) in air is larger by an order of magnitude than the root mean square height of the pavement texture. The tangential plane approximation developed for light scattering is not applicable in this case, but the perturbation solution *(5,14)* can be used to obtain the directional scattering pattern of ultrasonic waves.

One of the fundamental conclusions of the perturbation theory is that the scattering of monochromatic radiation by random surfaces, considered in the Fraunhofer zone, depends on only one harmonic of the surface continuum spectra. In other words, sound waves "see" a surface as having a periodic pattern of irregularities with one specific space frequency. By changing the direction of incident wave or viewing angle, different parts of the texture spectrum can be observed. The simple experiment described by Liebermann (*19*, p. 932) verifies the results of this theory. The scattering of ultrasound can

**TABLE 4 CALCULATED REFLECTANCE COEFFICIENTS (x $10^4$) FOR 1-DEGREE ANGLE OF REFLECTION**

| 0 | 2 | 5 | 10 | 15 | 20 | 25 | 30 | 45 | 60 | 75 | 90 | 105 | 120 | 135 | 150 | 165 |
|---|---|---|---|---|---|---|---|---|---|---|---|---|---|---|---|---|
| 346 | 346 | 346 | 346 | 346 | 346 | 346 | 346 | 346 | 346 | 346 | 346 | 346 | 346 | 346 | 346 | 346 |
| 391 | 391 | 391 | 390 | 388 | 385 | 382 | 379 | 366 | 351 | 336 | 323 | 312 | 303 | 296 | 291 | 288 |
| 428 | 428 | 426 | 422 | 415 | 407 | 397 | 386 | 352 | 319 | 291 | 269 | 252 | 238 | 228 | 221 | 218 |
| 454 | 453 | 450 | 441 | 426 | 408 | 389 | 369 | 314 | 269 | 234 | 206 | 186 | 171 | 160 | 152 | 148 |
| 467 | 465 | 459 | 441 | 415 | 387 | 360 | 334 | 268 | 217 | 178 | 149 | 128 | 113 | 102 | 95 | 91 |
| 467 | 462 | 452 | 423 | 387 | 352 | 321 | 293 | 223 | 170 | 130 | 102 | 83 | 70 | 61 | 55 | 52 |
| 455 | 448 | 433 | 392 | 350 | 312 | 280 | 252 | 182 | 130 | 93 | 68 | 52 | 41 | 34 | 30 | 28 |
| 435 | 426 | 405 | 356 | 310 | 273 | 243 | 216 | 148 | 98 | 64 | 44 | 31 | 23 | 18 | 16 | 14 |
| 412 | 400 | 373 | 318 | 273 | 238 | 210 | 184 | 119 | 73 | 44 | 27 | 18 | 13 | 10 | 8 | 7 |
| 362 | 344 | 307 | 249 | 210 | 181 | 157 | 133 | 76 | 38 | 19 | 10 | 6 | 4 | 3 | 2 | 2 |
| 314 | 290 | 248 | 196 | 164 | 140 | 118 | 97 | 47 | 20 | 8 | 4 | 2 | 1 | 1 | 0 | 0 |
| 272 | 244 | 200 | 156 | 130 | 110 | 90 | 70 | 28 | 10 | 3 | 1 | 1 | 0 | 0 | 0 | 0 |
| 236 | 204 | 163 | 125 | 104 | 87 | 68 | 51 | 17 | 5 | 2 | 1 | 0 | 0 | 0 | 0 | 0 |
| 206 | 172 | 134 | 103 | 86 | 69 | 52 | 36 | 10 | 2 | 1 | 0 | 0 | 0 | 0 | 0 | 0 |
| 181 | 146 | 111 | 86 | 70 | 55 | 39 | 26 | 6 | 1 | 0 | 0 | 0 | 0 | 0 | 0 | 0 |
| 160 | 124 | 93 | 73 | 59 | 44 | 30 | 19 | 3 | 1 | 0 | | | | | | |
| 165 | 101 | 44 | 22 | 16 | 12 | 12 | 10 | | | | | | | | | |
| 142 | 196 | 79 | 62 | 49 | 35 | 22 | 13 | 2 | 0 | | | | | | | |
| 127 | 92 | 68 | 53 | 41 | 28 | 17 | 10 | 1 | | | | | | | | |
| 114 | 80 | 59 | 46 | 35 | 22 | 13 | 7 | 1 | | | | | | | | |
| 102 | 70 | 51 | 40 | 29 | 18 | 10 | | | | | | | | | | |
| 93 | 61 | 45 | 35 | 25 | 14 | 7 | | | | | | | | | | |
| 85 | 54 | 40 | 31 | 21 | 12 | | | | | | | | | | | |
| 78 | 48 | 36 | 28 | 18 | 9 | | | | | | | | | | | |
| 71 | 43 | 32 | 24 | 15 | 8 | | | | | | | | | | | |
| 66 | 39 | 29 | 22 | 13 | 6 | | | | | | | | | | | |
| 61 | 34 | 26 | 19 | 11 | 5 | | | | | | | | | | | |
| 56 | 31 | 24 | 17 | 9 | | | | | | | | | | | | |
| 52 | 29 | 21 | 15 | 8 | | | | | | | | | | | | |
| 48 | 26 | 20 | 14 | 7 | | | | | | | | | | | | |

be used to obtain information on the pavement surface texture spectra. Then, by inverse Fourier analysis, a statistical height distribution of surface texture can be calculated.

Using the scale-modeling equipment available at MTC, simple experiments were done to correlate the skid resistance of pavements with the intensity of ultrasound backscattering. An electric spark was used as a high-intensity source of ultrasonic radiation, which was scattered from the 15-cm (6-in.) core samples. On the receiving side, 1/4-in. microphones were used to pick up the ultrasound. The signal was amplified, the particular frequency filtered, and the intensity of the filtered ultrasonic radiation measured. A detailed description of the experiments and equipment can be found elsewhere *(20, 21)*.

In these trial experiments, only major changes in the surface roughness and not the fine features of the surface texture were observed. The increase in surface roughness affects all spacial frequencies of the texture and so increases the intensity of ultrasonic backscattering. Thus a positive correlation is expected between pavement skid resistance and the intensity of backscattering.

The results of this experiment are shown in Figure 7 in which the ratio of the intensity of backscattering to the intensity of incident radiation is plotted against the skid number. The two plots on the graph are for two different frequencies of ultrasound. These frequencies are actually centers of the 1/3-octave band of filtered radiation. As was expected, a definite positive correlation between backscattering and skid resistance of the pavement surfaces may be observed in the figure.

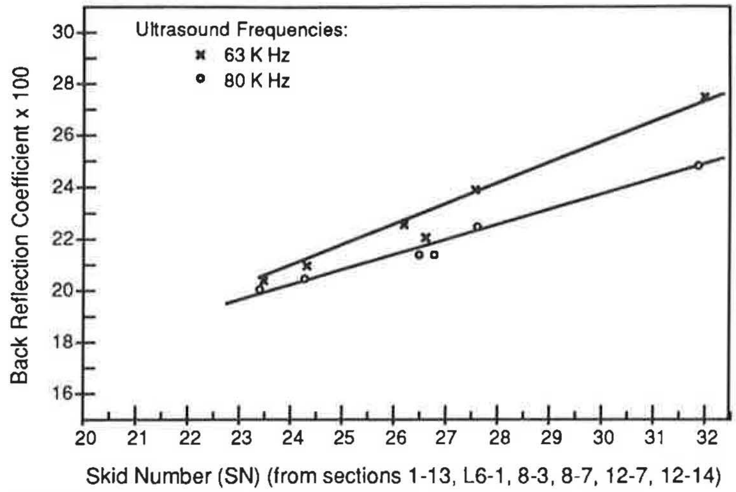


**FIGURE 7 Reflection of ultrasound by pavements of different roughness.**

## CONCLUSIONS AND RECOMMENDATIONS

The developed model and the experimental data obtained accurately explain observed reflectance properties of pavement. Furthermore, the results suggest that reflectance data can also be used for texture analysis. More detailed experimental investigations are needed to define the correlation between reflectance and pavement composition, as well as between reflectance and other pavement properties that depend on pavement texture.

Use of even higher reflection angles would permit more meaningful data to be obtained in such experiments because the influence of shadowing at high angles has only insignificant effects on results. This would permit simplification of the model and allow the use of distribution functions other than the Gaussian without introduction of unknown errors.

The use of ultrasonic waves for investigation of texture properties requires development of more suitable equipment than that used in the present study. However, even in the simple experiments conducted, a correlation of ultrasonic backscattering with skid resistance data was observed.

The results obtained in the experiments and model described suggest that a detailed analysis of the statistical properties of pavement texture is feasible by means of wave-scattering experiments.

## REFERENCES


1. IES Roadway Lighting Committee. Proposed American National Standard Practice for Roadway Lighting. *Journal of the Illuminating Engineering Society,* Vol. 12, No. 3, April 1983, pp. 146–196.
2. F. W. Jung, A. L. Kazakov, and A. Titishov. Road Surface Reflectance Measurements in Ontario. In *Transportation Research Record 996,* TRB, National Research Council, Washington, D.C., 1984, pp. 24–37.
3. F. W. Jung, A. L. Kazakov, and A. Titishov. *Road Surface Reflectance Measurements in Ontario.* Research and Development Branch, Ontario Ministry of Transportation and Communications, Downsview, Ontario, Canada, 1983.
4. A. L. Kazakov. *A Model for Predicting the Reduced Reflectance Coefficient Matrix.* Research and Development Branch, Ontario Ministry of Transportation and Communications, Downsview, Ontario, Canada, 1983.
5. S. Rayleigh. *The Theory of Sound.* 2 vols., London, 1896.
6. E. Feinberg. On the Propagation of Radio Waves Along an Imperfect Surface. *Journal of Physics,* Vol. 8, No. 6, 1944, pp. 317–330.
7. S. Rice. Reflection of Electromagnetic Waves from Slightly Rough Surfaces. *Communications on Pure and Applied Mathematics,* Vol. 4, 1951, pp. 351–378.
8. L. M. Brekhovskikh. Wave Diffraction at a Rough Surface. *Journal of Experimental and Theoretical Physics,* Vol. 3, 1952, pp. 375–304.
9. M. A. Isakovich. Wave Dispersion from a Randomly Uneven Surface. *Journal of Experimental and Theoretical Physis,* Vol. 3, No. 9, 1952, pp. 305–314.
10. F. G. Bass. Boundary Conditions for Average Electromagnetic Field on the Random Surface with the Random Fluctuation of the Impedance. *Radiophysica,* Vol. 3, No. 1, 1960, pp. 72–78.
11. B. F. Kur'yanov. The Scattering of Sound at a Rough Surface with Two Types of Irregularities. *Acoustics,* Vol. 8, No. 3, 1963, pp. 252–257.
12. B. I. Semenov. Approximate Computation of Scattering of Electromagnetic Waves by Rough Surface Contours. *Radiotechnica and Electronica,* Vol. 11, No. 8, 1966, pp. 1351–1361.
13. P. Beckmann and A. Spizzichino. *The Scattering of Electromagnetic Waves from Rough Surfaces.* Pergamon Press, Elmsford, N.Y., 1963.
14. F. G. Bass and I. M. Fucks. *The Scattering of Waves from Random Rough Surfaces* (in Russian). Nauka, Moscow, USSR, 1972.
15. M. I. Sancer. Shadow-Corrected Electromagnetic Scattering from a Randomly Rough Surface. *IEEE Transactions on Antennas and Propagation,* Vol. AP–17, No. 5, Sept. 1969.
16. J. A. Stratton. *Electromagnetic Theory.* McGraw-Hill Book Co., New York, 1941.
17. W. Gutt and P. J. Nixon. Studies of the Texture of Some Roadstone Materials by Scanning Electron Microscopy. *Journal of Material Science,* Vol. 7, 1972, pp. 995–1002.
18. I. S. Gradshtein and I. M. Rijick. *The Tables of Integrals, Sums, Series and Products* (in Russian). Nauka, Moscow, USSR, 1971.
19. L. N. Liebermann. Analysis of Rough Surfaces by Scattering. *Journal of Acoustical Society of America,* Vol. 35, No. 6, 1963.
20. A. L. Kazakov and C. Blaney. *The Scattering of Ultrasound by Pavement Surfaces.* Research and Development Branch, Ontario Ministry of Transportation and Communications, Downsview, Ontario, Canada, 1985.
21. M. N. Osman. *MTC Scale Model Facility for Transportation Noise Problems: Instrumentation Manual.* Report 77-AC-03. Research and Development Branch, Ontario Ministry of Transportation and Communications, Downsview, Ontario, Canada, June 1977.


*Publication of this paper sponsored by Committee on Visibility.*